

53 GBd PAM-4 DAC-LESS LOW-POWER (1.5 pJ/b) SILICON INTEGRATED TRANSMITTER

*Joris Lambrecht¹, Jochem Verbist^{1,2,3}, Hannes Ramon¹, Michael Vanhoecke¹,
Bart Moeneclaey¹, Laurens Bogaert^{1,2}, Peter Ossieur¹, Joris Van Campenhout⁴,
Johan Bauwelinck¹, Gunther Roelkens², Xin Yin¹*

¹*Ghent University-imec, IDLab, INTEC, 9052 Ghent, Belgium*

²*Ghent University – imec, Photonics Research Group, INTEC, 9052 Ghent, Belgium*

³*Current affiliation: BiFAST, 9000 Ghent, Belgium*

⁴*imec, Silicon Photonics group, 3001 Leuven, Belgium*

joris.lambrecht@ugent.be

Keywords: TRANSMITTER, PAM-4, SILICON PHOTONICS, ELECTRO-ABSORPTION MODULATOR

Abstract

We present an integrated PAM-4 transmitter consisting of two parallel GeSi electro-absorption modulators wirebonded to a SiGe BiCMOS driver, consuming 160mW excluding laser. 53GBd PAM-4 transmission is demonstrated over more than 1km fiber and 2km non-zero dispersion-shifted fiber, without using equalization or digital signal processing.

1 Introduction

Recent 400 Gigabit Ethernet (GbE) standards, e.g. 400GBASE-DR4, specify 53.125 GBd PAM-4 per lane up to 500m standard single-mode fiber (SSMF) for datacenter optical interconnects [1]. Longer fiber reaches up to 10 km are proposed in e.g. the 400GBASE-FR4 specifications [2]. These applications require high-bandwidth, linear PAM-4 transceivers in a very compact form factor and with low power consumption. Several PAM-4 transmitters have been demonstrated at or above 50 GBd [3-12]. Furthermore ref. [5] demonstrates a real-time 56 GBd PAM-4 link up to 2 km SSMF, but at 8.6W power consumption (excluding laser). However, [3-5] are based on long, travelling-wave Mach-Zehnder modulators (MZMs), which typically occupy a lot of area (several mm²) in the transceiver, even when monolithically integrated with the driver [13]. These traveling-wave structures typically require 50Ω terminations in the driver(s) and on the PIC, increasing the TX power consumption considerably. More compact single-modulator solutions, e.g. electro-absorption modulated lasers (EAMs)[6], and directly modulated lasers (DMLs)[7] often rely on power-hungry electrical digital-to-analog converters (DACs) to produce a (predistorted) PAM-4 signal which has to be linearly converted into the optical domain by the modulator. These transmitters typically use significant digital signal processing (DSP) at the TX or RX, or both. In [8], 56 GBd PAM-4 was transmitted with a single electro-absorption modulator (EAM) driven by an electrical DAC and RF-amplifier while using transmitter (TX) and receiver (RX) DSP, resulting in bit error ratios (BERs) below the HD-FEC threshold (3.8×10^{-3}) up to 2 km SSMF. In [9], a single microring modulator (MRR) and an integrated laser are combined with a low-power (160 mW) CMOS driver with on-chip compensation for the MRR characteristics. This resulted in 56 GBd PAM-4 with a very good eye quality, however without fiber transmission or BER. Out of [3-14], only [10], [11-12] and [14] utilize PAM-4 generation in the

optical domain (optical DAC). In [10], up to 64 GBd PAM-4 is demonstrated with a segmented microring resonator (MRR), without driver. In [14], a low-power transmitter is demonstrated based on flip-chip integration of a CMOS driver on a segmented MZM, but it is limited to 28 GBd. In [12], we demonstrated 64 GBd PAM-4 transmission over 1 km SSMF in real-time, using a parallel configuration of NRZ-driven EAMs. However a combination of RF-probes, an analog TX FFE (850 mW) and RF-amplifiers (5W) was used to drive the EAMs, due to the lack of an EAM driver IC. In this paper, a photonic integrated circuit (PIC) from imec's iSiPP50G platform with parallel EAMs incorporated in a Mach-Zehnder interferometer (MZI) is wirebonded to a very low-power EAM driver IC [15], implemented in 55 nm SiGe BiCMOS. The PIC contains a tunable optical power splitter and two lumped, unterminated EAMs, as was proposed in [11] but not yet implemented in [12]. The linearity requirements are removed from both driver and modulator, resulting in a low TX power consumption of only 160 mW (excluding laser), including the DC power dissipated in the heaters on the PIC (less than 15 mW). The EAMs are very compact, each EAM occupying only 120x180 μm² including metal routing and bondpads. BERs below or close to the KP4-FEC-threshold (2.4×10^{-4}) are shown for transmission of 53 GBd PAM-4 at 1565 nm across more than 1 km of SSMF and 2 km of non-zero dispersion-shifted fiber (NZ-DSF), while consuming only 1.5 pJ/b and occupying 0.275x1.72 mm² on the PIC and 0.75x1.2 mm² on the EIC.

2 Experiment setup

The measurement setup is illustrated in Fig. 1. The operation principle of the transmitter, described in detail in [11] and [12], is shown in Fig. 2. Two PRBS 2⁹-1 pseudo-random bit sequences (PRBS) at 53 Gb/s, produced by a 92 GSa/s arbitrary waveform generator (AWG) and decorrelated by introducing a relative delay (of at least 20 symbol periods) in the AWG, are sent directly through a 6-inch multi-coax cable

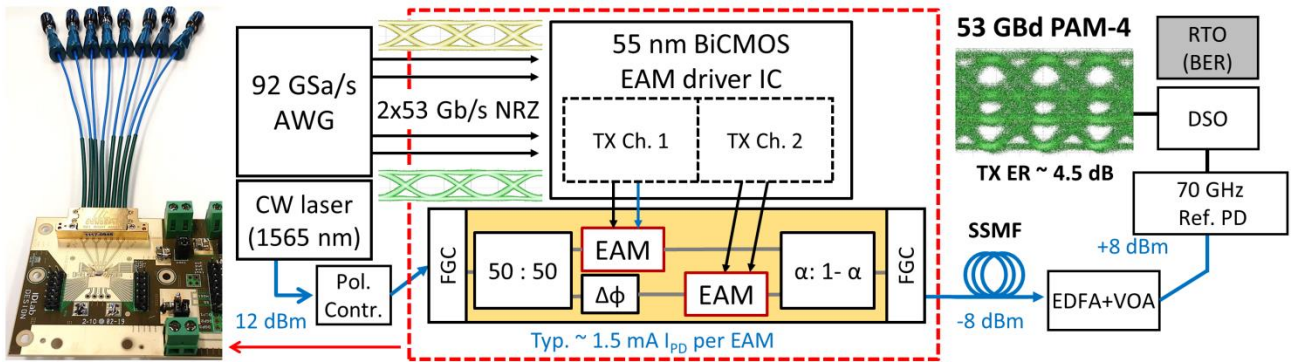


Fig. 1. Experiment setup.

assembly and RF-PCB transmission lines to the differential inputs of two driver channels in the TX electrical IC (EIC). The TX EIC non-linearly amplifies the input signals and drives the EAMs with up to 2 V_{pp} differential swing. The wirebond length towards the EAMs is minimized in the assembly to improve bandwidth and reduce bondwire-induced peaking (see Fig. 2). The external laser, set to 12 dBm at 1565 nm, is coupled into and out of the PIC through fiber-to-chip grating couplers (FGCs, 6 dB loss/FGC). Coupling loss can be improved to 2 dB per coupler with edge couplers [15]. A 50/50 power splitter is used at the input, ensuring that the EAMs receive equal optical power and behave as identical loads towards the driver IC. One branch is

phase-shifted ($\Delta\phi$ in Fig. 1-2) w.r.t. the other branch with a thermo-optic phase shifter. By default, the driver EIC biases both EAMs identically at approx. -1V, resulting in approximately 1.5mA DC photocurrent per EAM. The insertion loss per EAM was approximately 5 dB. Next, the modulated light is recombined using a tunable power combiner (implemented as a balanced MZI). Nominally the MZI is set to 33/66-operation ($\alpha=1/3$, Fig. 1-2), theoretically resulting in equidistant PAM-4 after power detection by the photodetector (PD) (Fig. 2) [11]. Thanks to the tunable recombination, up to 1.25 dB OMA improvement is expected w.r.t. an electrically weighted equivalent, as shown in [12]. After transmission over SSMF, an Erbium-doped fiber amplifier (EDFA) is used to overcome the insertion loss of the FGCs and as part of the reference receiver, which further consists of a variable optical attenuator (VOA) and a 70 GHz PD. The PD output is captured by a digital sampling oscilloscope (DSO) for eye diagrams, or by a 63 GHz 160 GSa/s real-time oscilloscope (RTO) for offline BER measurements. BER is measured directly after resampling, without using DSP.

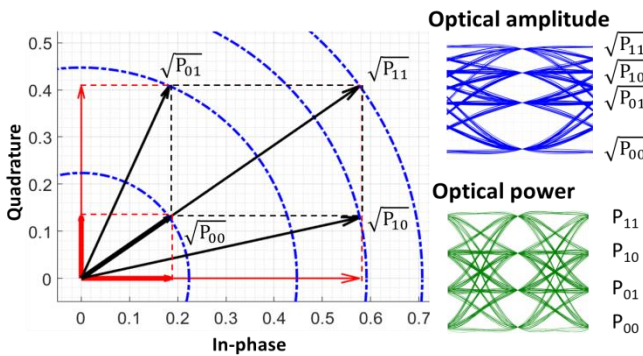


Fig. 2. PAM-4 transmitter principle, with $\Delta\phi=90^\circ$ and $\alpha=1/3$.

3 Results

In Fig. 4, the TX eyes diagrams, measured with the reference RX, are plotted vs. data rate. The TX outer extinction ratio

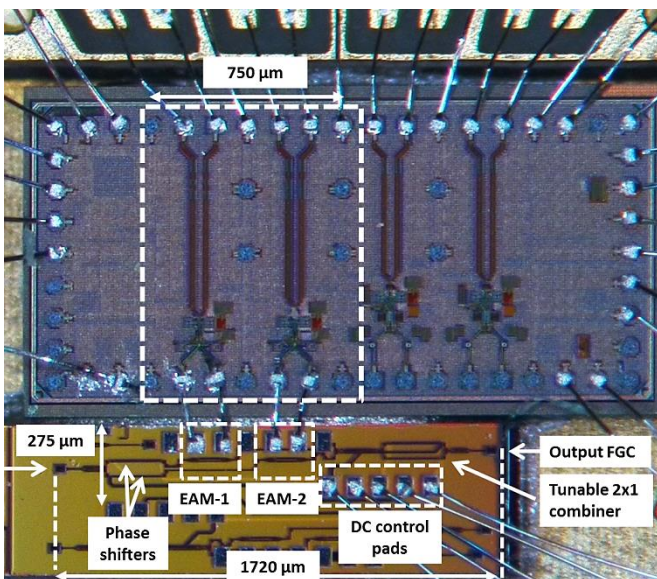


Fig. 3. Wirebonded PAM-4 TX.

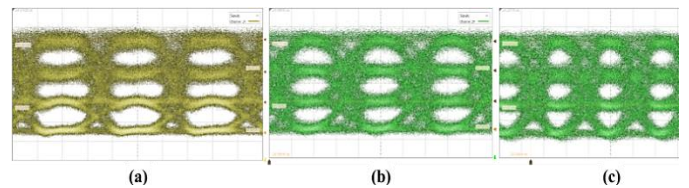


Fig. 4. TX output at (a) 28GBd (12ps/div, 15mV/div); (b) 40GBd (8ps/div, 15mV/div) and (c) 53GBd (8 ps/div, 16 mV/div).

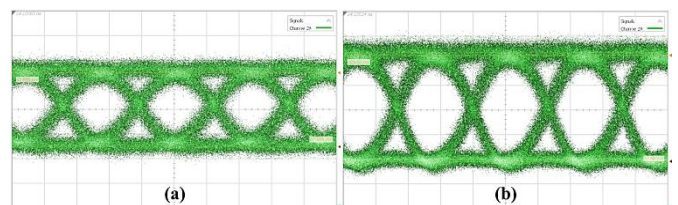


Fig. 5. TX NRZ outputs at 53 Gb/s. (a) LSB, 10 mV/div, 8 ps/div (b) MSB, 12 mV/div, 8 ps/div.

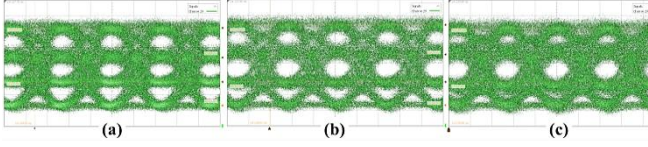


Fig. 6. 53GBd TX output vs. SSMF fiber length: no predistortion ($\alpha \approx 1/3$) (a) 0 km, (b) 0.5 km (c) 1 km

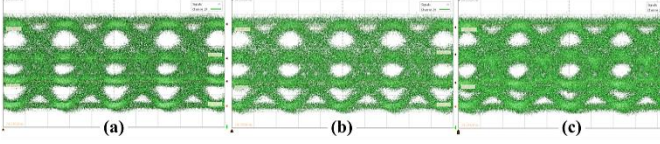


Fig. 7. 53GBd TX output vs. SSMF fiber length: predistorted ($\alpha < 1/3$) (a) 0 km, (b) 0.5 km (c) 1 km

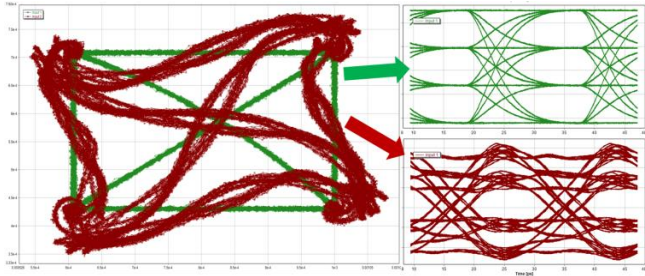


Fig. 8. Simulated TX output constellations and eye diagrams in back-to-back and with 1 km fiber.

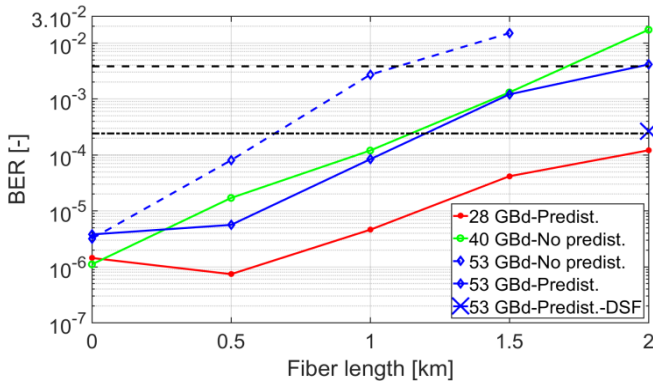


Fig. 9. TX BER vs. fiber length

(P_{11}/P_{00} , Fig. 2) is 5.3 dB at 28 GBd, and 4.5 dB at 40 GBd and 53 GBd. For comparison, the 53 GBd NRZ eyes, obtained by driving only MSB or LSB, are shown in Fig. 5. In Fig. 6-7, the 53GBd TX eyes diagrams, measured with the reference RX, are plotted vs. fiber length. Fig. 6. (a) shows the back-to-back TX output, optimized to obtain equidistant PAM-4 ($\alpha \approx 1/3$ with $\alpha:1-\alpha$ the power combination ratio of the tunable MZI). Chromatic dispersion results in, among other effects, symmetrical compression of the outer PAM-4 eyes which significantly increases the BER. VPI[®] simulation confirms this behaviour: with increasing fiber length, the outer edges of the constellation diagram are rotated w.r.t. its original center, which is located in the upper right quadrant of the complex plane (Fig. 2). This does not significantly affect $P_{11}-P_{00}$, but primarily reduces the eye opening in the outer eyes after detection by the PD. The tunable MZI on the PIC can be used to compensate this effect by changing only the DC heater voltage (and hence α in Fig. 1), which predistorts the TX PAM-4 output. This results in Fig. 7. As shown in Fig. 9, this improves the BER by approx. one order of magnitude and almost doubles the sub-KP4-FEC fiber reach

to approx. 1.25 km. Only a minimal BER penalty is observed in the back-to-back case: at 53GBd, a back-to-back BER of 3.77×10^{-6} is obtained with predistortion vs. a BER of 3.17×10^{-6} for the equidistant case. However without MZI predistortion, the BER increases above the KP4-threshold beyond 500m, whereas with predistortion, the BER at 1 km SSMF is still 8.3×10^{-5} . With 2km SSMF, a BER of 4.1×10^{-3} is measured, just above the HD-FEC threshold (3.8×10^{-3}). With 2 km NZ-DSF (single point), the BER is 2.62×10^{-4} , just above KP4-FEC. At 40 GBd, the back-to-back TX BER (unpredistorted) decreases to 1.1×10^{-6} , but the BER increase vs. fiber length is similar to the unpredistorted 53 GBd case. Except for the 40GBd back-to-back case (1.1×10^{-6}), the BER at 53GBd with predistortion is better than at 40GBd without predistortion. For 28GBd with predistortion, the back-to-back BER (1.43×10^{-6}) is slightly higher than the BER minimum of 7.35×10^{-7} at 500m, due to the predistortion which results in a smaller center eye. For 28GBd, the BER is below KP4-FEC beyond 2km SSMF (1.2×10^{-4}), and below HD-FEC up to 3.5 km SSMF (1.9×10^{-3}). Table 1 summarizes the state of the art on integrated PAM-4 transmitters. Compared to single-modulator solutions, the TX generates PAM-4 optically from two NRZ-driven EAMs. Therefore no linear drivers are required and the non-linearity of the modulator does not need to be compensated (as in [17]), which can reduce the power consumption of the TX significantly. Compared to classical MZM-based transmitters [13], even with very compact MZMs ($\sim 750 \mu\text{m}$ length in [14]), the TX is very low-power and compact, occupying only $0.275 \times 1.72 \text{ mm}^2$ on the PIC.

Ref.	Data rate [GBd]	Power [pJ/b]	TDECQ [dB]	BER [-]
[13]	25	30	-	-
[17]	28	18	-	10^{-6}
[14]	28/25	1.59**	-	$-/2 \times 10^{-5*}$
[9]	56	1.42**	0.5	-
This work	53	1.5***	-	3.17×10^{-6}

Table 1. State-of-the art integrated PAM-4 transmitters

*At 25 GBd. 28 GBd BER > KP4-FEC due to RX.

** Excluding heater(s) or temp. control. *** Including heaters

4 Conclusion

We have presented a 53 GBd silicon integrated PAM-4 optical transmitter, capable of sub-KP4-FEC BERs over up to more than 1 km SSMF at 1565 nm and a BER just above KP4-FEC with 2 km NZ-DSF, without using any equalization or DSP. Compared to the state of the art, the transmitter is both very compact and low-power (1.5 pJ/b).

5 Acknowledgements

The work was supported by EU H2020 projects Streams, Teraboard and Picture. The work of J. Lambrecht and H. Ramon was supported by the FWO.

6 References

- [1] "IEEE P802.3bs", <http://www.ieee802.org/3/bs>, Accessed 05/03/2019
- [2] "100G Lambda Multi-Source Agreement", <http://100glambda.com>, Accessed 05/03/2019
- [3] Chiuchiarelli, A., Ghandhi, R., Rossi, S. M. *et al.*, "Single wavelength 100G real-time transmission for high-speed data center communications," Proc. Opt. Fiber Comm. Conf. (OFC), Los Angeles, CA, USA, 2017, W14.2, pp. 1-3.
- [4] El-Fiky, El., Samani, A., Patel, D. *et al.*, "400 Gb/s O-band silicon photonic transmitter for intra-datacenter optical interconnects," *Opt. Express*, vol. 27, no. 7, pp. 10258-10268, April 2019.
- [5] Lee, J., Shahramian, S., Kaneda, N. *et al.*, "Demonstration of 112-Gbit/s Optical Transmission using 56GBaud PAM-4 Driver and Clock-and-Data Recovery ICs", Proc. European Conf. on Opt. Comm (ECOC), Valencia, Spain, 2015, DOI: 10.1109/ECOC.2015.7341667, pp. 1-3.
- [6] Nakai, Y., Nakanishi, A., Yamaguchi, Y. *et al.*, "Uncooled Operation of 53-Gbaud PAM4 (106-Gb/s) EA/DFB Lasers with Extremely Low Drive Voltage with 0.9 Vpp," Proc. European Conf. on Opt. Comm (ECOC), Rome, Italy, 2018, DOI: 10.1109/ECOC.2018.8535399, Mo4D.4, pp. 1-3.
- [7] Sasada, N., Nakajima, T., Sekino, Y. *et al.*, "Wide-temperature-range (25°C to 80°C) 53-Gbaud PAM4 (106-Gb/s) Operation of 1.3- μ m Directly Modulated DFB Lasers for 10-km Transmission", Proc. European Conf. on Opt. Comm (ECOC), Rome, Italy, 2018, PDP, pp. 1-3.
- [8] El-Fiky, E., De Heyn, P., Osman, M. *et al.*, "112 Gb/s PAM4 Transmission over 2 km SMF Using a C-band GeSi Electro-Absorption Modulator," Proc. Opt. Fiber Comm. Conf. (OFC), San Diego, CA, 2018, W2A.16, pp. 1-3.
- [9] Li, H., Balamurugan, G., Sakib, M., *et al.*, "A 112 Gb/s PAM4 Transmitter with Silicon Photonics Microring Modulator and CMOS Driver", Proc. OFC 2019, Th4A.4, San Diego, USA, 2019
- [10] Sun, J., Kumar, R., Sakib, M. *et al.*, "A 128 Gb/s PAM4 Silicon Microring Modulator With Integrated Thermo-Optic Resonance Tuning", in *Journal of Lightwave Technology*, vol. 37, no. 1, pp. 110-115, 1 Jan.1, 2019. doi: 10.1109/JLT.2018.2878327
- [11] Verbist, J., Lambrecht, J., Verplaetse, M. *et al.*, "DAC-less and DSP-free PAM-4 Transmitter at 112 Gb/s with Two Parallel GeSi Electro-Absorption Modulators," 2017 European Conference on Optical Communication (ECOC), Gothenburg, 2017, pp. 1-3. doi: 10.1109/ECOC.2017.8346098
- [12] Verbist, J., Lambrecht, J., Verplaetse, M. *et al.*, "Real-Time and DSP-Free 128 Gb/s PAM-4 Link Using a Binary Driven Silicon Photonic Transmitter" in *Journal of Lightwave Technology*, vol. 37, no. 2, pp. 274-280, 15 Jan.15, 2019. doi: 10.1109/JLT.2018.2877461
- [13] Rito, P., Lopez, I.G., Petousi, D. *et al.*, "A Monolithically Integrated Segmented Linear Driver and Modulator in EPIC 0.25- μ m SiGe:C BiCMOS Platform," in *IEEE Transactions on Microwave Theory and Techniques*, vol. 64, no. 12, pp. 4561-4572, Dec. 2016.
- [14] Tanaka, S., Takasi, S., Aoki, T. *et al.*, "Ultralow-Power (1.59 mW/Gbps), 56-Gbps PAM4 Operation of Si Photonic Transmitter Integrating Segmented PIN Mach-Zehnder Modulator and 28-nm CMOS Driver", in *Journal of Lightwave Technology*, vol. 36, no. 5, pp. 1275-1280, March 1, 2018. doi: 10.1109/JLT.2018.2799965
- [15] Ramon, H., Lambrecht, J., Verbist, J. *et al.*, "70 Gb/s Low-Power DC-coupled NRZ Differential Electro-Absorption Modulator Driver in 55 nm SiGe BiCMOS," in *Journal of Lightwave Technology*, vol. 37, no. 5, pp. 1504-1514, 1 March, 2019. doi: 10.1109/JLT.2019.2900192
- [16] Snyder, B., Mangal, N., Lepage, G. *et al.*, "Packaging and Assembly Challenges for 50G Silicon Photonics Interposers," Proc. Opt. Fiber Comm. Conf. (OFC), San Diego, CA, 2018, Tu2A.3, pp. 1-3.
- [17] Kishi, T., Nagatani, M., Kanazawa, S. *et al.*, "56-Gb/s Optical Transmission Performance of an InP HBT PAM4 Driver Compensating for Nonlinearity of Extinction Curve of EAM," in *Journal of Lightwave Technology*, vol. 35, no. 1, pp. 75-81, 1 Jan.1, 2017. doi: 10.1109/JLT.2016.2624778